

# Perturbation of membrane dynamics in nerve cells as an early event during bilirubin-induced apoptosis

Cecília M. P. Rodrigues,<sup>1,\*</sup> Susana Solá,<sup>\*</sup> Rui E. Castro,<sup>\*</sup> Pedro A. Laires,<sup>\*</sup> Dora Brites,<sup>\*</sup> and José J. G. Moura<sup>†</sup>

Centro de Patogénese Molecular,<sup>\*</sup> Faculdade de Farmácia, University of Lisbon, 1600-083 Lisbon; and Departamento de Química,<sup>†</sup> Faculdade de Ciências e Tecnologia, Universidade Nova de Lisboa, 2825-114 Monte de Caparica, Portugal

**Abstract** Increased levels of unconjugated bilirubin, the end product of heme catabolism, impair crucial aspects of nerve cell function. In previous studies, we demonstrated that bilirubin toxicity may be due to cell death by apoptosis. To characterize the sequence of events leading to neurotoxicity, we exposed developing rat brain astrocytes and neurons to unconjugated bilirubin and investigated whether changes in membrane dynamic properties can mediate apoptosis. Bilirubin induced a rapid, dose-dependent increase in apoptosis, which was nevertheless preceded by impaired mitochondrial metabolism. Using spin labels and electron paramagnetic resonance spectroscopy analysis of whole cell and isolated mitochondrial membranes exposed to bilirubin, we detected major membrane perturbation. By physically interacting with cell membranes, bilirubin induced an almost immediate increase in lipid polarity sensed at a superficial level. The enhanced membrane permeability coincided with an increase in lipid fluidity and protein mobility and was associated with significant oxidative injury to membrane lipids. In conclusion, apoptosis of nerve cells induced by bilirubin is mediated by its primary effect at physically perturbing the cell membrane. Bilirubin directly interacts with membranes influencing lipid polarity and fluidity, protein order, and redox status. **Key words:** These data suggest that nerve cell membranes are primary targets of bilirubin toxicity.—Rodrigues, C. M. P., S. Solá, R. E. Castro, P. A. Laires, D. Brites, J. J. G. Moura. **Perturbation of membrane dynamics in nerve cells as an early event during bilirubin-induced apoptosis.** *J. Lipid Res.* 2002. 43: 885–894.

**Supplementary key words** bilirubin neurotoxicity • cell death • electron paramagnetic resonance spectroscopy • membrane lipid and protein structure • oxidative stress • spin labels

Neonatal hyperbilirubinemia is frequently observed in newborns within the first week following birth due to the transient accumulation of bilirubin, a bile pigment formed during the catabolism of heme (1). In some cases, however, especially in infants who are premature and/or have associated hemolytic disorders, abnormal accumulation of bilirubin in the central nervous system is a cause of bilirubin encephalopathy, which may contribute to increased morbidity and adverse neurologic sequelae (1, 2).

Despite our increasing understanding of the toxic effects of bilirubin on various crucial aspects of cell function, the sequence of events leading to bilirubin neurotoxicity is still poorly understood. Several studies have demonstrated that bilirubin may modulate DNA and protein synthesis (3–6), neurotransmitter synthesis, and release and uptake (7–10), and protein phosphorylation (8, 11–13). Moreover, there is now experimental evidence that apoptosis may play a crucial role in bilirubin cytotoxicity (14–16). In this regard, we have recently shown that bilirubin induces cytochrome *c* release in developing rat brain neurons, in a process associated with caspase-3 activation and poly(ADP-ribose) polymerase (PARP) cleavage, requiring mitochondrial depolarization, together with Bax translocation (17). Furthermore, bilirubin-induced apoptosis may also occur via activation of *N*-methyl-D-aspartate (NMDA) receptors, as it has been described in vivo using the Gunn rat model (18) and recently confirmed in vitro using rat brain neurons (14). These cellular manifestations of bilirubin toxicity have been ascribed, in part, to its affinity for membrane lipids (19–22), thus changing membrane lipid composition (23) and modifying lipid order in erythrocytes (24) and mitochondria (25). In addition, transfer of bilirubin from its complex with plasma albumin and precipitation of bilirubin diacid with phosphatidylcholine in nerve cell membranes has been suggested to account for neurotoxicity (26). Few studies, however, have concentrated on further clarifying the molecular and physical basis of interactions between bilirubin and nerve cell membranes.

The present study is intended to characterize the sequence of events leading to bilirubin neurotoxicity, from interaction with membranes to impairment of metabolic function and ultimately cell death. Plasma and mitochon-

Abbreviations: EPR, electron paramagnetic resonance; NS, nitroxyl stearate.

<sup>†</sup>To whom correspondence should be addressed.  
e-mail: cmprodriues@ff.ul.pt

drial membrane structural changes associated with bilirubin-induced apoptosis in nerve cells were investigated by using a sensitive electron paramagnetic resonance (EPR) spectroscopy technique of spin labeling. This experimental approach characterizes dynamic properties along fatty acid chains and in proteins, as well as oxidative injury to membrane lipids. The results demonstrate enhanced membrane permeability concomitant with decreased lipid and protein order, and significant oxidative damage in nerve cells exposed to bilirubin. All these changes, occurring in the region closer to the polar head groups, were observed very rapidly after treatment with bilirubin, thus preceding biochemical and morphological manifestations of apoptosis. This study provides novel insight into the mechanism of bilirubin-mediated apoptosis of neural cells, while offering new prospects for prevention and treatment of bilirubin encephalopathy.

## MATERIALS AND METHODS

### Materials

General laboratory chemicals were obtained from Merck (Darmstadt, Germany) and Sigma Chemical Co. (St. Louis, MO). For cell culture, fetal calf serum, Hank's balanced salt solutions (HBSS), B-27 Supplement, DMEM, and Neurobasal medium were obtained from Life Technologies Inc. (Grand Island, NY). Tissue culture plates were from Corning Costar Corp. (Cambridge, MA). For mitochondria isolation, Percoll was obtained from Sigma Chemical Co., and Chelex-100 resin (potassium form) was from Bio-Rad Laboratories (Hercules, CA). Unconjugated bilirubin, also from Sigma Chemical Co., was purified according to McDonagh and Assisi (27). Hoechst dye 33258, 3-(4,5-dimethylthiazol-2-yl)-2,5-diphenyltetrazolium bromide (MTT), and spin labels 5-nitroxyl stearate (5-NS), 7-NS, 12-NS, 16-NS, and 4-maleimido-2,2,6,6-tetramethylpiperidinoxyl (4-maleimido-TEMPO) were obtained from Sigma Chemical Co.

### Isolation and culture of rat primary astrocytes and neurons

Astrocytes were isolated from 2-day-old Wistar rats as described previously (28), with minor modifications. Briefly, the rat brain was collected after decapitation in DMEM containing 11 mM sodium bicarbonate, 71 mM glucose, and 1% antibiotic and antimycotic solution. Meninges, blood vessels, and white matter were then removed. The cortex was homogenized by mechanical fragmentation, and the cell suspension passed sequentially through steel screens of 230, 104, and 73.3  $\mu\text{m}$  pore size. Cells were collected by centrifugation at 700  $g$  for 10 min and resuspended in DMEM supplemented with 10% FBS. Finally,  $2 \times 10^5$  cells/ $\text{cm}^2$  were plated and maintained at 37°C in a humidified atmosphere of 5%  $\text{CO}_2$ . The medium was replaced at day 7, and confluent cultures were used after 10 days in culture. Cells were morphologically characterized by phase contrast microscopy, and by indirect immunocytochemistry for glial fibrillary acidic protein.

Rat neurons were isolated from fetuses of 17–18 days pregnant Wistar rats as previously described (29) with minor modifications. In short, pregnant rats were ether anesthetized and decapitated. The fetuses were collected in HBSS-1 and rapidly decapitated. After removal of meninges and white matter, the brain cortex was collected in HBSS-2, mechanically fragmented, transferred to a 0.025% trypsin in HBSS-2 solution, and incubated for

15 min at 37°C. Following trypsinization, cells were washed twice in HBSS-2 containing 10% FBS, and resuspended in Neurobasal medium supplemented with 0.5 mM L-glutamine, 25  $\mu\text{M}$  L-glutamic acid, 2% B-27 Supplement, and 12 mg/ml gentamicin. Aliquots of  $1 \times 10^5$  cells/ $\text{cm}^2$  were plated on tissue culture plates pre-coated with poly-D-lysine, and maintained at 37°C in a humidified atmosphere of 5%  $\text{CO}_2$ . Every 3 days, 0.5 ml of old medium was replaced by fresh medium without glutamic acid, and confluent cultures were used after 8 days in culture. Neurons were morphologically characterized by phase contrast microscopy, and by indirect immunocytochemistry for neurofilaments. All animals received humane care according to the criteria outlined in the "Guide for the Care and Use of Laboratory Animals" prepared by the national Academy of Sciences and published by the National Institutes of Health (NIH publication 86-23 revised 1985).

### Induction of apoptosis, morphologic analysis, and MTT metabolism

Isolated rat astrocytes and neurons were cultured as described above and then exposed for 0.5, 1, 4, 8, and 24 h to 0.9, 4.3, and 8.6  $\mu\text{M}$  unconjugated bilirubin. Bilirubin was dissolved in dimethylsulfoxide immediately prior to use and kept under light protection throughout the experiments. Appropriate controls treated with dimethylsulfoxide vehicle only (<1%) were also included. The medium was gently removed at the end of each incubation period and scored for nonviable cells by trypan blue dye exclusion, while attached cells were fixed for morphologic evaluation of apoptotic changes. In brief, cells were fixed with 4% formaldehyde in PBS, pH 7.4, for 10 min at room temperature, incubated with Hoechst at 5 mg/ml in PBS for 5 min, washed with PBS and mounted using PBS-glycerol (3:1, v/v). Fluorescence was visualized using a Axioskop<sup>®</sup> fluorescence microscope (Carl Zeiss GmbH, Jena, Germany). Fluorescent nuclei were scored by different people and categorized according to the condensation and staining characteristics of chromatin. Normal nuclei showed non-condensed chromatin dispersed over the entire nucleus. Apoptotic nuclei were identified by condensed chromatin, contiguous to the nuclear membrane, as well as nuclear fragmentation of condensed chromatin. Three random microscopic fields per sample of approximately 200 nuclei were counted and mean values expressed as the percentage of apoptotic nuclei.

In addition, we used the MTT tetrazolium salt assay to assess mitochondrial metabolic function, since mitochondrial enzymes normally have the capacity to transform MTT tetrazolium salt into MTT formazan (30). In brief, MTT tetrazolium salt was dissolved in serum-free culture medium (0.5 mg/ml) and added to cells for 1 h at 37°C. The medium was then removed, isopropanol/0.04 M HCl was added, and MTT formazan crystals dissolved with gentle shaking. The absorbance was measured at 570 nm and the results expressed as percentage of control.

### Cell harvesting and sub-cellular fractionation prior to spectroscopic analysis

Astrocytes and neurons were removed from tissue culture plates by trypsinization, and the resulting suspensions were pelleted, washed, and either incubated directly with spin labels in PBS, pH 7.4, or subjected to sub-cellular fractionation for mitochondria isolation. In brief, cells were homogenized in an ice-cold solution of 70 mM sucrose, 220 mM mannitol, 1 mM EGTA, and 10 mM HEPES, pH 7.4 as a 10% (w/v) homogenate. The homogenate was centrifuged at 600  $g$  for 10 min at 4°C, and the post-nuclear supernatant further centrifuged at 7,000  $g$  for 10 min at 4°C. The crude mitochondrial pellet was then purified by sucrose-Percoll gradient centrifugation at 43,000  $g$  for 20 min at

4°C using a 20 ml self-generating gradient containing 0.25 M sucrose, 1 mM EGTA, and Percoll (75:25, v/v). The lower turbid layer was resuspended in 30 ml of wash buffer containing 0.1 M KCl, 5 mM 3-(*N*-morpholino)-propane sulfonic acid (MOPS), and 1 mM EGTA, pH 7.4, and centrifuged at 7,000 *g* for 10 min at 4°C. The resulting mitochondrial pellet was washed twice more using the same buffer, and a final wash was carried out in chelex-100-treated buffer (200–400 mesh, potassium form) without EGTA. The pellet was suspended in chelex-100-treated resuspension buffer containing 125 mM sucrose, 50 mM KCl, 5 mM HEPES, and 2 mM KH<sub>2</sub>PO<sub>4</sub>. Following isolation, mitochondria were maintained on ice and used for experiments within 3 h of isolation. Aliquots were removed for examining the purity of the mitochondria preparation as previously described (31). Protein content was determined using the Bio-Rad protein assay as recommended by the manufacturer.

### Electron paramagnetic resonance spectroscopy and spin-labeling techniques

Changes in membrane lipid and protein structure can be measured by EPR spectroscopy using paramagnetic reporter groups incorporated into membranes, which give characteristic spectra upon excitation with microwaves in a magnetic field. Characteristics of plasma and mitochondrial membrane polarity at varying depths were examined by using three different NS probes (5-, 7-, and 16-NS), in which the paramagnetic center localizes at different positions along the hydrocarbon chain of the stearic acid molecule (32–34). Using the 5-NS membrane-associated probe, the nitroxide moiety resides near the lipid-water interface, while in the 16-NS it localizes deeper in the lipid bilayer. A reliable parameter of the environment of these spin labels, calculated from direct measurements of the parallel and perpendicular components of the hyperfine tensor of the spin label, is the isotropic splitting factor  $a_0$ . A high  $a_0$  reflects increased polarity of the lipid membrane. In addition, alterations in membrane fluidity of 5- and 7-NS spin labels, showing restricted motion in the membrane, were evaluated by measuring the outer half-width at half-height of the low-field extreme ( $\Delta I$ ). The larger  $\Delta I$ , the more motion and less order in the local microenvironment reported by the nitroxide group. This parameter is more sensitive than the classical parameter  $S$ , and is independent from changes in the polarity of the environment around the nitroxide, thus rendering corrections unnecessary (35, 36). For the 16-NS spin label, which showed a higher degree of motional freedom, the ratio of the height of the low-field and the center-field line ( $h_{+1}/h_0$ ) was used as an empirical measurement of membrane lipid organization (37, 38). An increased ratio reflects a decrease in membrane organization. In addition, we used the 4-maleimido-TEMPO label, which binds to the sulfhydryl group of proteins giving information about mobility of protein reactive groups and allowing the measurement of changes in structure of protein-rich membranes (34, 39, 40). The ratio of the height of the midline to the height of the high-field line of the spectrum ( $h_0/h_{-1}$ ) reflects the freedom of motion of this label at its binding site, and thus provides a parameter for the mobility of thiol groups within the membrane. A high ratio indicates a low freedom of motion.

All spin labels were dissolved in chloroform, separated into 2- $\mu$ g aliquots, evaporated under nitrogen, and left under vacuum for at least 2 h. Intact cells and freshly isolated mitochondria (60–80  $\mu$ g protein) were incubated in spin-label coated tubes with gentle shaking for 90 min at 37°C (5-, 7-, 16-NS), or for 1 min at 22°C (4-maleimido-TEMPO), yielding systems containing approximately 2 mol spin label per 100 mol membrane lipids (2 mol% probe). In these conditions, the incorporation of the spin label into the membrane was constant, while distortion of the

spectra due to spin-spin interaction was not noticed. Moreover, levels of incorporation were controlled by double integration of the spectra, thus assuring that results are independent of the spin-label concentration.

Membrane lipid peroxidation in intact cells and isolated mitochondria was also assessed using electron paramagnetic resonance as described previously (41–43). In brief, membranes (60–80  $\mu$ g protein) were incubated with two membrane-associated, oxidation-sensitive, paramagnetic nitroxyl stearate probes (12- $\mu$ g aliquots), 5-NS and 12-NS, with gentle agitation for 20 min at 22°C. The incorporation of these spin probes into membranes results in characteristic EPR spectra, since increased production of reactive oxygen species causes loss of paramagnetism of the spin label and hence loss of signal amplitude, measured as the height of the center-field line of the spectrum, providing that the shape remains the same.

Labeled membranes were then exposed to either unconjugated bilirubin (0.9, 4.3, and 8.6  $\mu$ M), or dimethylsulfoxide vehicle (control) in PBS, pH 7.4, for 5, 15, and 60 min at 22°C. At the end of each exposure period, membrane suspensions were spun down at 12,000 *g* for 3 min, and the pellet used for EPR spectroscopy analysis. After resuspension in PBS (60  $\mu$ l), pellets were sucked into 100  $\mu$ l glass capillaries, sealed at both ends, and the capillaries introduced within standard 4-mm quartz tubes containing silicone oil for thermal stability. All spectra were acquired at 9.8 GHz (X-band) on a Bruker EMX electron paramagnetic resonance spectrometer (Bruker, Karlsruhe, Germany)

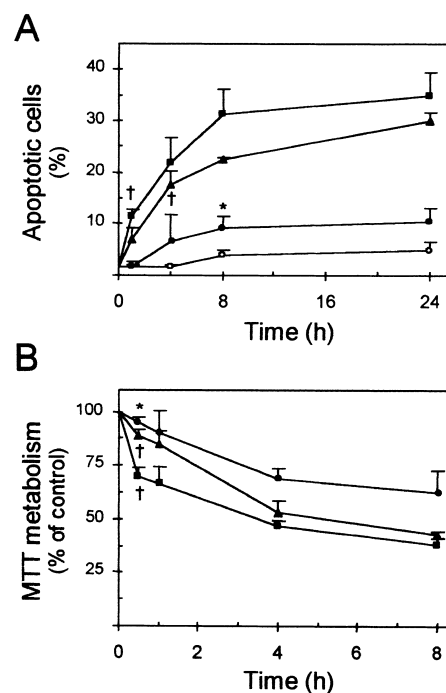


**Fig. 1.** Bilirubin induces death of cortical astrocytes. Cells were isolated and cultured for 8 days prior to incubation with either vehicle (control; open circles), 0.9  $\mu$ M (closed circles), 4.3  $\mu$ M (triangles), or 8.6  $\mu$ M (squares) unconjugated bilirubin as described in Materials and Methods. A: Apoptosis of astrocytes assayed by Hoechst staining and expressed as percentage of total cells. B: Mitochondrial function of astrocytes assessed by the 3-(4,5-dimethylthiazol-2-yl)-2,5-diphenyltetrazolium bromide (MTT) assay and expressed as percentage of controls. All values are mean  $\pm$  SEM of at least three separate experiments. \* $P < 0.05$  and † $P < 0.01$  from control at the same time point.

using a rectangular cavity (model ER 4102ST) and 100 kHz field modulation frequency, 1.05 G modulation amplitude, and 20 mW microwave power at 22°C.

### Statistical analysis

Fold and percent changes were calculated based on corresponding controls. All data are expressed as mean  $\pm$  SEM from at least three separate experiments. Differences between groups were compared using the unpaired two-tailed Student's *t*-test, performed on the basis of equal or unequal variance as appropriate, and *P* values lower than 0.05 were considered statistically significant.

## RESULTS

### Unconjugated bilirubin induces rapid apoptosis in nerve cells

Nerve cells were incubated in the presence of unconjugated bilirubin at low micromolar concentrations for 1, 4, 8, and 24 h, and examined for the characteristic morphologic nuclear changes associated with apoptosis using Hoechst staining. Similar results were obtained when cell viability was assessed by trypan blue dye exclusion (data not shown). As expected, the percentage of apoptotic glial cells detected in controls after 1 h was negligible, increasing

only slightly at 24 h (Fig. 1A). Bilirubin caused a dose-dependent cell killing with a relatively rapid onset. Depending on the concentration, only up to 10% of astrocytes died within the first hour following bilirubin exposure. This percentage, however, stretched up to 22% at 4 h, 31% at 8 h, and 35% at 24 h. Interestingly, the most striking increase in apoptosis usually occurred at 4 h with only smaller changes at latter time points. A dose- and time-dependent cell death by apoptosis was also evident in neurons, although with a  $\sim$ 30% increased susceptibility of neurons versus astrocytes (*P* > 0.01).

### Bilirubin-induced cell death is preceded by loss of mitochondrial metabolic function

As judged by the decreased ability to metabolize MTT to formazan, bilirubin caused a dose- and time-dependent loss of mitochondrial function that preceded apoptosis in nerve cells. In fact, only 30 min following exposure of astrocytes to 0.9, 4.3, and 8.7  $\mu$ M bilirubin, MTT metabolism was already reduced to 95, 89, and 70% of control, respectively (Fig. 1B). Moreover, mitochondrial function was impaired by 30–50% within the first 4 h of exposure but further inhibition of MTT metabolism was marginal at 8 h. Note that the loss of viability indicated by morphologic analysis of Hoechst

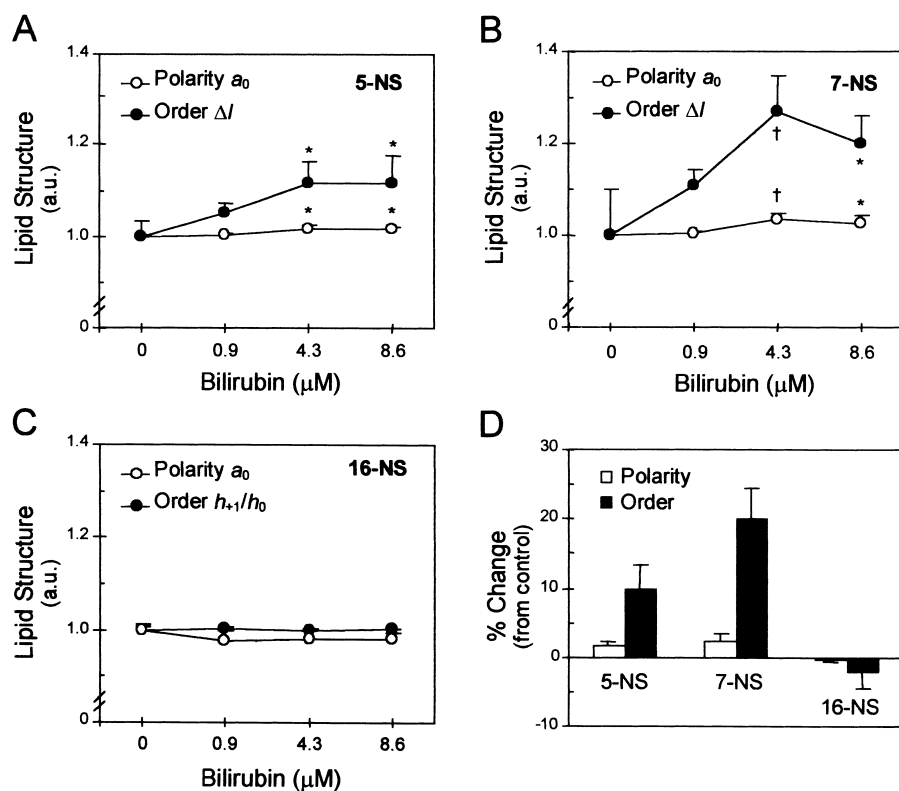


**Fig. 2.** Concentration-dependent changes in lipid structure induced by bilirubin in whole astrocyte membranes. Cell membranes were labeled with either 5-nitroxyl stearate (NS), 7-NS, or 16-NS spin probes, exposed to unconjugated bilirubin for 5 min, and examined for permeability and fluidity by electron paramagnetic resonance (EPR) spectroscopy analyses as described in Materials and Methods. A, B, C: Dose-response to bilirubin-induced alteration in lipid polarity ( $a_0$ ) and order ( $\Delta I$  or  $h_{+1}/h_0$ ) throughout various depths within the membrane bilayer. Labeled cells were incubated with either bilirubin (0.9, 4.3, and 8.6  $\mu$ M), or no addition (0  $\mu$ M; control). D: Percent change in lipid polarity and order induced by 4.3  $\mu$ M bilirubin. Values are mean  $\pm$  SEM relative to controls of at least three separate experiments. \**P* < 0.05 and †*P* < 0.01 from control.

staining is less pronounced than that displayed in the MMT assay. This may indeed reflect a decrease in mitochondrial metabolism in a subpopulation of cells that will not undergo apoptosis and later recover their metabolic function.

### Changes in lipid and protein structure of intact nerve cell membranes occurs almost immediately after exposure to bilirubin

Several hypotheses point to the cell membrane as a possible primary target of bilirubin neurotoxicity. To determine if bilirubin interaction modifies lipid structure in intact nerve cells, primary rat astrocytes and neurons were labeled with the NS spin probes 5-, 7-, and 16-NS and then exposed to unconjugated bilirubin at different concentrations. **Figure 2** shows changes in  $a_0$ ,  $\Delta I$ , and  $h_{+1}/h_0$  during incubation of labeled astrocyte membranes with bilirubin. Treatment of intact glial cells with the lowest bilirubin concentration for 5 min did not alter lipid fluidity or polarity, irrespective of the probe used. However, 4.3  $\mu\text{M}$  bilirubin (0.25 mg/dl) caused significant 10% and 20% increases in  $\Delta I$ , sensed by 5-NS and 7-NS, respectively, indicating a less ordered lipid bilayer organization. Increases in lipid polarity were also detectable, although less pronounced, using 5-NS and 7-NS spin probes. 16-NS labeling

of intact astrocyte membranes did not reveal significant changes in spectral parameters, which was in great contrast with moderated and marked increases, respectively, in polarity and fluidity at carbon numbers 5 and 7, respectively. Thus, unconjugated bilirubin promotes membrane permeabilization and decreases phospholipid order closer to the membrane-water interface, but it does not alter membrane properties in more hydrophobic regions, greatly suggesting a superficial interaction.

Having verified that significant membrane perturbation in astrocytes occurred using 4.3  $\mu\text{M}$  bilirubin, we selected this concentration to evaluate alterations in membrane dynamic properties as a function of time (**Fig. 3**). Maximum effects on spin-label microenvironment polarity and order were found after 15 min of incubation using 5- and 7-NS probes, while longer periods did not further change, or even slightly reduce, the influence of bilirubin on lipid membrane properties. This is in line with both a deeper location and increased aggregation of bilirubin after longer incubation periods reported previously (24). In addition, when the motion parameter was expressed as percentage of control for each spin label, we detected 10% and 17% increased fluidity at C-5 after 5 min and 15 min of incubation, respectively ( $P < 0.05$ ). Moreover, greater perturbation was evident at C-7, where lipid motion was

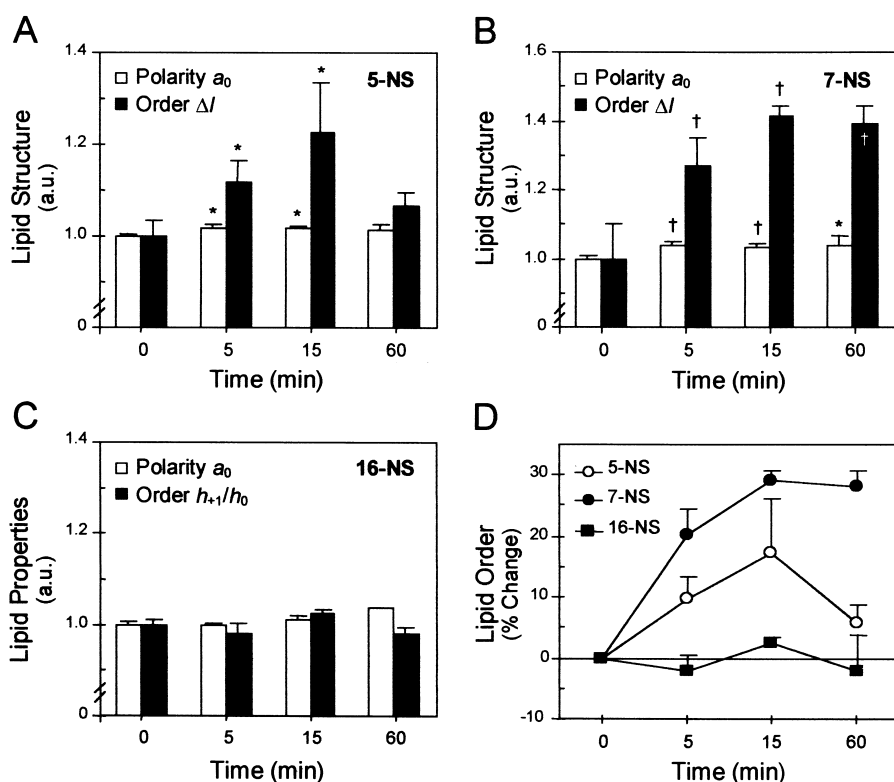


**Fig. 3.** Time-dependent changes in lipid structure induced by bilirubin in whole astrocyte membranes. Cell membranes were labeled with either 5-NS, 7-NS, or 16-NS spin probes, exposed to 4.3  $\mu\text{M}$  unconjugated bilirubin and examined for permeability and fluidity by EPR spectroscopy analyses as described in Materials and Methods. A, B, C: Time-course of bilirubin-induced alteration in lipid polarity ( $a_0$ ) and order ( $\Delta I$  or  $h_{+1}/h_0$ ) throughout various depths within the membrane bilayer. Labeled cells were incubated with bilirubin for either 0, 5, 15, or 60 min. D: Percent change in lipid order induced by bilirubin. Values are mean  $\pm$  SEM relative to controls of at least three separate experiments. \* $P < 0.05$  and † $P < 0.01$  from control.

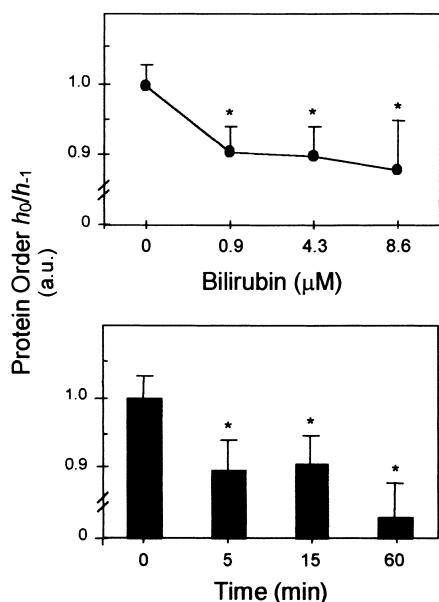


**Fig. 4.** Concentration- and time-dependent changes in protein motion induced by bilirubin in whole astrocyte membranes. Cell membranes were labeled with 4-maleimido-TEMPO spin probe, exposed to unconjugated bilirubin, and examined for protein order ( $h_0/h_{-1}$ ) by EPR spectroscopy analyses as described in Materials and Methods. Labeled cells were incubated with either bilirubin (0, 0.9, 4.3, and 8.6  $\mu\text{M}$ ) for 5 min (top), or 4.3  $\mu\text{M}$  bilirubin for 0, 5, 15, and 60 min (bottom). Values are mean  $\pm$  SEM relative to controls of at least three separate experiments. \* $P < 0.05$  from control.

20% and 30% greater than in controls at the same time points ( $P < 0.01$ ). Corroborating the information given above, the parameter  $a_0$  followed a similar trend (Fig. 3). The unlikely hypothesis that phospholipids are extensively extracted by bilirubin was tested and, as expected, the stronger signal in the membrane pellet as compared with the supernatant indicated little extraction of spin labels. Most importantly, signal intensities in the buffer following incubation with the bilirubin molecule were similar to those of respective controls (data not shown).

Using the protein-oriented spin label 4-maleimido-TEMPO, we found that the mobility parameter  $h_0/h_{-1}$  was already significantly decreased using 0.9  $\mu\text{M}$  bilirubin for 5 min ( $P < 0.05$ ), and continued to decrease slightly using greater concentrations and longer incubation periods (Fig. 4). These changes reflect an increased mobility of the spin label and may be explained by disruption of the ordered structure of astrocyte membrane proteins induced by bilirubin.

We finally investigated the interaction of unconjugated bilirubin with intact neurons and compared the results with those described above using astrocytes. As shown in Fig. 5, 3.4  $\mu\text{M}$  bilirubin during 5 min influences lipid fluidity and protein order of glial and neuronal cell membranes in a similar manner, despite the increased sensitivity of neurons to cell death by apoptosis. In fact, the 7-NS spin label shows approximately 25% increased motion in neurons against 20% in astrocytes, whereas the 4-maleimido-TEMPO reflects 10% decreased protein order in both cell types. It is, there-

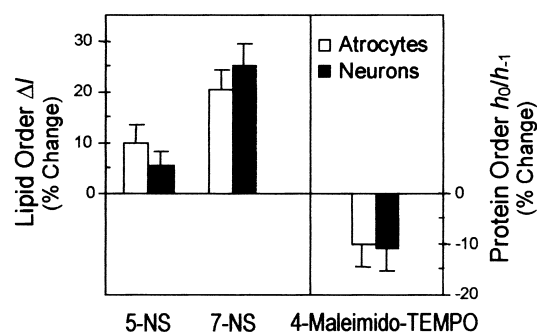


**Fig. 5.** Percent change in lipid and protein motion induced by bilirubin in whole glial and neuronal cell membranes. Cell membranes were labeled with either 5-NS, 7-NS, or 4-maleimido-TEMPO spin probes, exposed to 4.3  $\mu\text{M}$  unconjugated bilirubin for 5 min, and examined for lipid ( $\Delta l$ ) and protein ( $h_0/h_{-1}$ ) order by EPR spectroscopy analyses as described in Materials and Methods. Values are mean  $\pm$  SEM relative to controls of at least three separate experiments.

fore, possible that astrocytes have better intracellular defense mechanisms than neurons, given the otherwise similar interaction of bilirubin with glial and neuronal cell membranes.

#### Oxidative injury to lipids of intact nerve cell membranes accompanies changes in membrane structure

To determine if exposure to bilirubin modifies levels of cell membrane oxidation, astrocytes and neurons were probed with 5-NS and 12-NS spin labels and then exposed to unconjugated bilirubin. As depicted in Fig. 6A and B, bilirubin caused a rapid, dose-dependent loss of 5-NS spin-probe intensity, manifested by a decrease in peak amplitude. Treatment of glial cells with 0.9  $\mu\text{M}$  bilirubin for 5 min already significantly altered 5-NS signal amplitude, while 4.3 and 8.6  $\mu\text{M}$  concentrations caused 15% and 17% decreases in spin-probe intensity, respectively ( $P < 0.01$ ). Decreases in signal amplitude were slightly more marked at 15 min of incubation, but remained unchanged for a subsequent 60-min incubation period (data not shown). The magnitude of the 12-NS signal incorporated into astrocyte membranes was hardly decreased during exposure to bilirubin, indicative of less damage in deeper regions of the bilayer. Using a different methodological approach to measure signal intensity, based on the double integration of 5-NS and 12-NS spectra, we confirmed the results described above (data not shown). Finally, spin-label signal amplitude was also assessed in neurons in the presence of bilirubin (Fig. 6C). Treatment of 5-NS-labeled neuronal cell membranes with bilirubin resulted in decreased signal amplitudes that were no different from those of astrocytes, indicating that bilirubin induces lipid peroxidation in nerve cell membranes irrespective of the cell type.

#### Bilirubin disrupts lipid polarity, protein order, and redox status also in mitochondrial membranes isolated from astrocytes

Mitochondrial membranes were purified from cultured astrocytes, loaded with 5-NS, 7-NS, and 4-maleimido-TEMPO, and then exposed to unconjugated bilirubin.

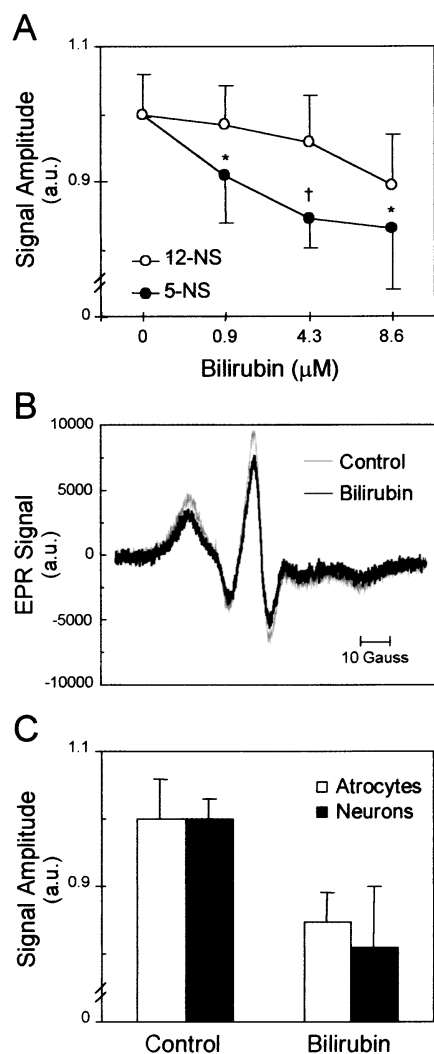


**Fig. 6.** Loss of spin-probe intensity induced by bilirubin in whole glial and neuronal cell membranes. Cell membranes were labeled with either 5-NS or 12-NS spin probes, exposed to unconjugated bilirubin for 5 min, and examined for reactive oxygen species production by EPR spectroscopy analyses as described in Materials and Methods. A: Dose-response to bilirubin-induced alteration in 5-NS and 12-NS signal amplitude. Labeled astrocytes were incubated with either bilirubin (0.9, 4.3, and 8.6  $\mu\text{M}$ ), or no addition (0  $\mu\text{M}$ ; control). B: Alteration in EPR spectra sensed by the 5-NS spin label after incubation of astrocytes with 4.3  $\mu\text{M}$  bilirubin. C: Changes in signal amplitude sensed by the 5-NS spin label after incubation of astrocytes and neurons with 4.3  $\mu\text{M}$  bilirubin. Values are mean  $\pm$  SEM relative to controls of at least three separate experiments. \* $P < 0.05$  and † $P < 0.01$  from control.

bin (Fig. 7). Consistent with altered mitochondrial function as assessed by the MTT assay, treatment with bilirubin caused a significant increase in lipid polarity sensed by 7-NS ( $P < 0.05$ ), together with a decrease in protein order ( $P < 0.05$ ). These data suggest a superficial interaction of bilirubin also with mitochondrial membranes, leading to increased membrane permeability. Mitochondria from astrocytes demonstrated very marked decreases ( $\sim 30\%$ ) in the 5-NS signal amplitude in response to bilirubin ( $P < 0.05$ ), indicative of a significant oxidative injury.

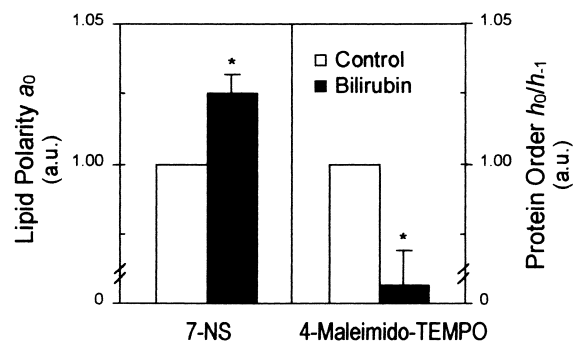


**Fig. 7.** Changes in lipid polarity and protein order induced by bilirubin in mitochondrial membranes isolated from astrocytes. Mitochondrial membranes were labeled with either 7-NS or 4-maleimido-TEMPO spin probes, exposed to 4.3  $\mu\text{M}$  unconjugated bilirubin for 5 min, and examined for lipid polarity ( $a_0$ ) and protein order ( $h_0/h_{-1}$ ) by EPR spectroscopy analyses as described in Materials and Methods. Values are mean  $\pm$  SEM relative to controls of at least three separate experiments. \* $P < 0.05$  from control.

## DISCUSSION

The present study shows that apoptosis induced by bilirubin in nerve cells is rapid but preceded by disruption of mitochondrial metabolism. Furthermore, almost immediately after exposure, unconjugated bilirubin interacts superficially with both whole nerve cell membranes and purified mitochondrial membranes, wherein it acts to significantly disrupt lipid polarity and fluidity, protein order, and redox status. These findings, when taken together with our prior studies showing morphologic and biochemical characteristics of apoptosis in cultured neural cells incubated with bilirubin (15–17), indicate that bilirubin-induced neurotoxicity is mediated, in part, by its primary effect of physically perturbing cell membranes.


Several mechanisms have been implicated in bilirubin neurotoxicity where both metabolic compromise and excitotoxicity appear to play a key role. In this regard, the activation of NMDA receptors has been described in vivo (18) and recently confirmed in vitro (14), while mitochondria are thought to be particularly vulnerable to bilirubin-mediated toxicity (44–46). Several studies have demonstrated abnormal energy metabolism in brain from hyperbilirubinemic rats (47) and depressed membrane potential in synaptosomal plasma membrane vesicles isolated from rat brain and incubated with bilirubin (48). We have also shown that exposure of isolated mitochondria to unconjugated bilirubin resulted in swelling and increased mitochondrial membrane permeability (15). Based on these previous observations regarding bilirubin toxicity, we have now extended our initial studies to show that 4.3  $\mu\text{M}$  bilirubin promotes neuronal cell death by apoptosis as early as after 1 h of exposure. The apoptotic process most likely involves cytochrome *c* release, caspase-3 activation, and PARP cleavage, and requires mitochondrial depolarization, together with Bax translocation (17). Thus, detection of cell dysfunction at earlier stages, before morphological and biochemical changes of apoptosis, is critical for understanding the pathways of programmed cell death.

An early event during apoptosis appears to be the acquisition of plasma membrane changes that allows macrophages to recognize and engulf these cells before any rupture. In fact, soon after initiating apoptosis, most mammalian cell types translocate phosphatidylserine from the inner face of the plasma membrane to the cell surface, which most likely reflects increased membrane fluidity. Furthermore, the release of apoptogenic factors from mitochondria requires increased membrane permeability. The nature of membrane changes that occur in apoptotic cells remains, however, poorly defined.

In the present study, we have provided evidence that low, clinically relevant concentrations of bilirubin (49–51) decrease neural cell viability in a rapid process that is nevertheless preceded by lipid polarity and fluidity changes in superficial membrane regions, thus reflecting a primary physical interaction. These structural effects were characterized using spin labeling techniques and further corroborated by expressing spectroscopic parameters as a percent change from control, since it surpasses the influence of polarity and order gradients along the depth of the membrane leaflet (33, 35, 52). A superficial interaction of bilirubin with membrane bilayers has been similarly proposed in other studies using erythrocyte membranes (24), sustaining the appearance of echinocytic forms, or model phospholipid bilayers (53–55). Conversely, a recent study using high-pressure, infrared spectroscopy of the solvation of bilirubin in lipid bilayers indicated that bilirubin intercalates into the polymethylene chain region of the bilayer, being located between the carbonyl region and the methylene group two carbons from the methyl terminus (56). Different methodological conditions, such as the use of biological whole cell membranes, resealed right-side-out ghosts, or artificial lipid bilayers, may account for conflicting observations published by different groups. For instance, the presence of proteins is one factor known to increase the partitioning of bilirubin into biological bilayers as compared with model bilayers of identical composition but lacking proteins (57). The distinct lipid and protein composition of nerve cells membranes may further account for the specificity of bilirubin interaction.

The increased motion in the nerve plasma membrane induced by unconjugated bilirubin as described above is also supported by the observation that bilirubin augments the mobility of the 4-maleimido-TEMPO label, indicating disruption of the protein order structure and increased membrane fluidity much above control values. Bilirubin-induced membrane permeabilization is equally evident in mitochondria isolated from nerve cells, confirming our previous studies using purified organelles (15, 25) and linking structural changes with the release of apoptogenic factors such as cytochrome *c*. Together with the partitioning properties of bilirubin demonstrated by this study, it is possible that subsequent lipid and protein rearrangement may cause additional changes of membrane fluidity. On a different note, we also document here increased lipid peroxidation during incubation of whole neural cells and isolated mitochondrial membranes with bilirubin in the  $\mu\text{M}$

range concentrations, which is consistent with the reported collapse of mitochondrial transmembrane potential in neurons exposed to bilirubin (17). Oxidative injury of specific lipids may be an additional factor contributing to increased membrane fluidity. Indeed, it has been shown that selective oxidation of phosphatidylserine usually occurs before any signs of cytotoxicity and precedes the externalization of phosphatidylserine during apoptosis (58).

In conclusion, perturbation of cell membrane structure represents an immediate component of the apoptotic pathway triggered by bilirubin, reinforcing the concept that membranes are primary targets of bilirubin neurotoxicity. Our data indicate that the superficial interaction of bilirubin with cell membranes likely accounts for a rapid disruption of membrane lipid polarity and fluidity, altered protein order, and increased oxidative injury, which precede metabolic and morphologic manifestations of apoptosis. Functionally, the increase in plasma membrane fluidity associated with apoptosis of nerve cells induced by bilirubin may represent a mechanism to cycle phosphatidylserine to the outer leaflet, perhaps mediating phagocytic recognition of apoptotic cells. Thus, new prospects for prevention and treatment of bilirubin encephalopathy should consider the use of molecules, such as the bile salt ursodeoxycholate, that by stabilizing cell membranes (15, 17) could prevent severe lesions during neonatal jaundice. 

The authors thank members of the laboratory for their comments and encouragement during the course of this work; Telmo Pedro for technical assistance; and Carlos Brondino from the Departamento de Química, FCT, Universidade Nova de Lisboa, Monte de Caparica, Portugal, for his expertise in the use of the electron paramagnetic resonance spectrometer. This work was supported in part by grant PRAXIS/C/SAU/14311/1998 from Fundação para a Ciência e a Tecnologia, Lisbon, Portugal (to C.M.P.R.).

Manuscript received 25 September 2001 and in revised form 28 January 2002.

## REFERENCES

1. Gourley, G. R. 1997. Bilirubin metabolism and kernicterus. *Adv. Pediatr.* **44**: 173–229.
2. Lee, K. S., and L. M. Gartner. 1986. Fetal bilirubin metabolism and neonatal jaundice. *In* Bile Pigments and Jaundice. J. D. Ostrow, editor. Marcel Dekker, New York. 373–394.
3. Majumdar, A. P. N. 1974. Bilirubin encephalopathy: effect on RNA polymerase activity and chromatin template activity in the brain of Gunn rat. *Neurobiology*. **4**: 425–431.
4. Yamada, N., Y. Sawasaki, and H. Nakajima. 1977. Impairment of DNA synthesis in Gunn rat cerebellum. *Brain Res.* **126**: 295–307.
5. Schiff, D., G. Chan, and M. J. Poznansky. 1985. Bilirubin toxicity in neuronal cell lines N-115 and NBR-10A. *Pediatr. Res.* **19**: 908–911.
6. Kashiwamata, S., S. Aono, and R. K. Semba. 1980. Characteristic changes of cerebellar proteins associated with cerebellar hypoplasia in jaundiced Gunn rats and the prevention of these by phototherapy. *Experientia*. **36**: 1143–1144.
7. Ohno, T. 1980. Kernicterus: effect on choline acetyltransferase, glutamic acid decarboxylase and tyrosine hydroxylase activities in the brain of Gunn rat. *Brain Res.* **196**: 282–285.
8. Hansen, T. W. R., D. Bratlid, and S. I. Walaas. 1988. Bilirubin de-



- creases phosphorylation of synapsin I, a synaptic vesicle-associated neuronal phosphoprotein, in intact synaptosomes from rat cerebral cortex. *Pediatr. Res.* **23**: 219–223.
9. Silva, R., L. R. Mata, S. Gulbenkian, M. A. Brito, C. Tiribelli, and D. Brites. 1999. Inhibition of glutamate uptake by unconjugated bilirubin in cultured cortical rat astrocytes: role of concentration and pH. *Biochem. Biophys. Res. Commun.* **265**: 67–72.
  10. Ochoa, E. L., R. P. Wennberg, Y. An, T. Tandon, T. Takashima, T. Nguyen, and A. Chui. 1993. Interactions of bilirubin with isolated presynaptic nerve terminals: functional effects on the uptake and release of neurotransmitters. *Cell Mol. Neurobiol.* **13**: 69–86.
  11. Morphis, L., A. Constantopoulos, N. Matsaniotis, and A. Papatophilis. 1982. Bilirubin-induced modulation of cerebral protein phosphorylation in neonate rabbits *in vivo*. *Science.* **218**: 156–158.
  12. Sano, K., H. Nakamura, and T. Matsuo. 1985. Mode of inhibitory action of bilirubin on protein kinase C. *Pediatr. Res.* **19**: 587–590.
  13. Hansen, T. W. R., S. B. Mathiesen, and S. I. Walaas. 1996. Bilirubin has widespread inhibitory effects on protein phosphorylation. *Pediatr. Res.* **39**: 1072–1077.
  14. Grojean, S., V. Koziel, P. Vert, and J. L. Daval. 2000. Bilirubin induces apoptosis via activation of NMDA receptors in developing rat brain neurons. *Exp. Neurol.* **166**: 334–341.
  15. Rodrigues, C. M. P., S. Solá, R. Silva, and D. Brites. 2000. Bilirubin and amyloid- $\beta$  peptide induce cytochrome *c* release through mitochondrial membrane permeabilization. *Mol. Med.* **6**: 936–946.
  16. Silva, R. F., C. M. P. Rodrigues, and D. Brites. 2001. Bilirubin-induced apoptosis in glial and nerve cells is aggravated by chenodeoxycholic acid but prevented by ursodeoxycholic acid. *J. Hepatol.* **34**: 402–408.
  17. Rodrigues, C. M. P., S. Solá, and D. Brites. 2002. Bilirubin induces apoptosis via the mitochondrial pathway in developing rat brain neurons. *Hepatology.* **36**: 335–341.
  18. McDonald, J. W., S. M. Shapiro, F. S. Silverstein, and M. V. Johnston. 1998. Role of glutamate receptor-mediated excitotoxicity in bilirubin-induced brain injury in the Gunn rat model. *Exp. Neurol.* **150**: 21–29.
  19. Mustafa, M. G., and T. E. King. 1970. Binding of bilirubin with lipid. A possible mechanism of its toxic reactions in mitochondria. *J. Biol. Chem.* **245**: 1084–1089.
  20. Hayward, D., D. Schiff, S. Fedunec, G. Chan, P. J. Davis, and M. J. Poznansky. 1986. Bilirubin diffusion through lipid membranes. *Biochim. Biophys. Acta.* **860**: 149–153.
  21. Ali, S., and D. Zakim. 1993. The effects of bilirubin on the thermal properties of phosphatidylcholine bilayers. *Biophys. J.* **65**: 101–105.
  22. Hansen, T., S. Tommarello, and J. Allen. 2001. Subcellular localization of bilirubin in rat brain after *in vivo* i.v. administration of [ $^3$ H]bilirubin. *Pediatr. Res.* **49**: 203–207.
  23. Brito, M. A., R. Silva, C. Tiribelli, and D. Brites. 2000. Assessment of bilirubin toxicity to erythrocytes. Implication in neonatal jaundice management. *Eur. J. Clin. Invest.* **30**: 239–247.
  24. Brito, M. A., C. D. Brondino, J. J. Moura, and D. Brites. 2001. Effects of bilirubin molecular species on membrane dynamic properties of human erythrocyte membranes: a spin label electron paramagnetic resonance spectroscopy study. *Arch. Biochem. Biophys.* **387**: 57–65.
  25. Rodrigues, C. M. P., S. Solá, M. A. Brito, D. Brites, and J. J. G. Moura. 2002. Bilirubin directly disrupts membrane lipid polarity and fluidity, protein order, and redox status in rat mitochondria. *J. Hepatol.* **36**: 335–341.
  26. Brodersen, R. 1979. Bilirubin. Solubility and interaction with albumin and phospholipid. *J. Biol. Chem.* **254**: 2364–2369.
  27. McDonagh, A. F., and F. Assisi. 1972. The ready isomerization of bilirubin IX- in aqueous solution. *Biochem. J.* **129**: 797–800.
  28. Blondeau, J. P., A. Beslin, F. Chantoux, and J. Francon. 1993. Triiodothyronine is a high-affinity inhibitor of amino acid transport system L1 in cultured astrocytes. *J. Neurochem.* **60**: 1407–1413.
  29. Brewer, G. J., J. R. Torricelli, E. K. Eeveg, and P. J. Price. 1993. Optimized survival of hippocampal neurons in B27-supplemented Neurobasal, a new serum-free medium combination. *J. Neurosci. Res.* **35**: 567–576.
  30. Mosmann, T. 1983. Rapid colorimetric assay for cellular growth and survival: application to proliferation and cytotoxicity assays. *J. Immunol. Methods* **65**: 55–63.
  31. Rodrigues, C. M. P., G. Fan, P. Y. Wong, B. T. Kren, and C. J. Steer. 1998. Ursodeoxycholic acid may inhibit deoxycholic acid-induced apoptosis by modulating mitochondrial transmembrane potential and reactive oxygen species production. *Mol. Med.* **4**: 165–178.
  32. Jost, P., L. J. Libertini, V. C. Hebert, and O. H. Griffith. 1971. Lipid spin labels in lecithin multilayers. A study of motion along fatty acid chains. *J. Mol. Biol.* **59**: 77–98.
  33. Harris, J., T. J. Power, A. L. Bieber, and A. Watts. 1983. An electron-spin-resonance spin-label study of the interaction of purified Mojave toxin with synaptosomal membranes from rat brain. *Eur. J. Biochem.* **131**: 559–565.
  34. Güldütuna, S., G. Zimmer, M. Leuschner, S. Bhatti, A. Elze, B. Deisinger, M. Hofmann, and U. Leuschner. 1999. The effect of bile salts and calcium on isolated rat liver mitochondria. *Biochim. Biophys. Acta.* **1453**: 396–406.
  35. Hubbell, W. L., and H. M. McConnell. 1971. Molecular motion in spin-labeled phospholipids and membranes. *J. Am. Chem. Soc.* **93**: 314–326.
  36. Mason, R. P., E. B. Giavedoni, and A. P. Dalmasso. 1977. Complement-induced decrease in membrane mobility: introducing a more sensitive index of spin-label motion. *Biochemistry.* **16**: 1196–1201.
  37. Schreier, S., W. A. Frezzatti, Jr., P. S. Araujo, H. Chaimovich, and I. M. Cuccovia. 1984. Effect of lipid membranes on the apparent pK of the local anesthetic tetracaine. Spin label and titration studies. *Biochim. Biophys. Acta.* **769**: 231–237.
  38. Bianconi, M. L., A. T. do Amaral, and S. Schreier. 1988. Use of membrane spin label spectra to monitor rates of reaction of partitioning compounds: hydrolysis of a local anesthetic analog. *Biochem. Biophys. Res. Commun.* **152**: 344–350.
  39. Lai, C. S., N. M. Tooney, and E. G. Ankel. 1984. Structure and flexibility of plasma fibronectin in solution: electron spin resonance spin-label, circular dichroism, and sedimentation studies. *Biochemistry.* **23**: 6393–6397.
  40. Kunicki, T. J., D. J. Nugent, R. S. Piotrowicz, and C. S. Lai. 1986. Covalent attachment of sulfhydryl-specific, electron spin resonance spin-labels to Fab' fragments of murine monoclonal antibodies that recognize human platelet membrane glycoproteins. Development of membrane protein specific spin probes. *Biochemistry.* **25**: 4979–4983.
  41. Butterfield, D. A., K. Hensley, M. Harris, M. Mattson, and J. Carney. 1994.  $\beta$ -Amyloid peptide free radical fragments initiate synaptosomal lipoperoxidation in a sequence specific fashion: implications to Alzheimer's disease. *Biochem. Biophys. Res. Commun.* **200**: 710–715.
  42. Hensley, K., J. Carney, N. Hall, W. Shaw, and D. A. Butterfield. 1994. Electron paramagnetic resonance investigations of free radical-induced alterations in neocortical synaptosomal membrane protein infrastructure. *Free Radic. Biol. Med.* **17**: 321–331.
  43. Bruce-Keller, A. J., J. G. Begley, W. Fu, D. A. Butterfield, D. E. Bredesen, J. B. Hutchins, K. Hensley, and M. P. Mattson. 1998.  $\beta$ -Amyloid peptide free radical fragments initiate synaptosomal lipoperoxidation in a sequence specific fashion: implications to Alzheimer's disease. *J. Neurochem.* **70**: 31–39.
  44. Cowger, M. L., R. P. Igo, and R. F. Labbe. 1965. The mechanism of bilirubin toxicity studied with purified respiratory enzyme and tissue culture systems. *Biochemistry.* **4**: 2763–2770.
  45. Mustafa, M. G., M. L. Cowger, and T. E. King. 1969. Effects of bilirubin on mitochondrial reactions. *J. Biol. Chem.* **244**: 6403–6414.
  46. Noir, B. A., A. Boveris, A. M. Garaza Pereira, and A. O. Stoppani. 1972. Bilirubin: a multi-site inhibitor of mitochondrial respiration. *FEBS Lett.* **27**: 270–274.
  47. Batty, H. K., and O. E. Millhouse. 1976. Ultrastructure of the Gunn rat substantia nigra. II. Mitochondrial changes. *Acta. Neuropathol. (Berl)*. **34**: 7–19.
  48. Mayor, F. Jr., J. Diez-Guerra, F. Valdivieso, and F. Mayor. 1986. Effect of bilirubin on the membrane potential of rat brain synaptosomes. *J. Neurochem.* **47**: 363–369.
  49. Bratlid, D. 1990. How bilirubin gets into the brain. *Clin. Perinatol.* **17**: 449–465.
  50. Mayor, F. Jr., M. Pages, J. Diez-Guerra, F. Valdivieso, and F. Mayor. 1985. Effect of postnatal anoxia on bilirubin levels in rat brain. *Pediatr. Res.* **19**: 231–236.
  51. Ostrow, J. D., and C. Tiribelli. 2001. New concepts in bilirubin

neurotoxicity and the need for studies at clinically relevant bilirubin concentrations. *J. Hepatol.* **34**: 467–470.

52. Fretten, P., S. J. Morris, A. Watts, and D. Marsh. 1980. Lipid-lipid and lipid-protein interactions in chromaffin granule membranes. A spin label ESR study. *Biochim. Biophys. Acta.* **598**: 247–259.
53. Zucker, S. D., J. Storch, M. L. Zeidel, and J. L. Gollan. 1992. Mechanism of the spontaneous transfer of unconjugated bilirubin between small unilamellar phosphatidylcholine vesicles. *Biochemistry.* **31**: 3184–3192.
54. Cestaro, B., G. Cervato, S. Ferrari, G. Di Silvestro, D. Monti, and P. Manitto. 1983. Interaction of bilirubin with small unilamellar vesicles of dipalmitoylphosphatidylcholine. *Ital. J. Biochem.* **32**: 318–329.
55. Zucker, S. D., W. Goessling, E. J. Bootle, and C. Sterritt. 2001. Localization of bilirubin in phospholipid bilayers by parallax analysis of fluorescence quenching. *J. Lipid Res.* **42**: 1377–1388.
56. Zakim, D., and P. T. A. Wong. 1990. A high-pressure, infrared spectroscopic study of the solvation of bilirubin in lipid bilayers. *Biochemistry.* **29**: 2003–2007.
57. Leonard, M., N. Noy, and D. Zakim. 1989. The interactions of bilirubin with model and biological membranes. *J. Biol. Chem.* **264**: 5648–5652.
58. Kagan, V. E., J. P. Fabisiak, A. A. Shvedova, Y. Y. Tyurina, V. A. Tyurin, N. F. Schor, and K. Kawai. 2000. Oxidative signaling pathway for externalization of plasma membrane phosphatidylserine during apoptosis. *FEBS Lett.* **477**: 1–7.